ACCOUNTS
of chemical research

Construction and Optoelectronic Properties of Organic One-Dimensional Nanostructures

YONG SHENG ZHAO, HONGBING FU, AIDONG PENG, YING MA, QING LIAO, AND JIANNIAN YAO*

Beijing National Laboratory for Molecular Sciences, CAS Key Laboratory of Photochemistry, Institute of Chemistry, Chinese Academy of Sciences, Beijing 100190, China

RECEIVED ON JULY 31, 2009

CONSPECTUS

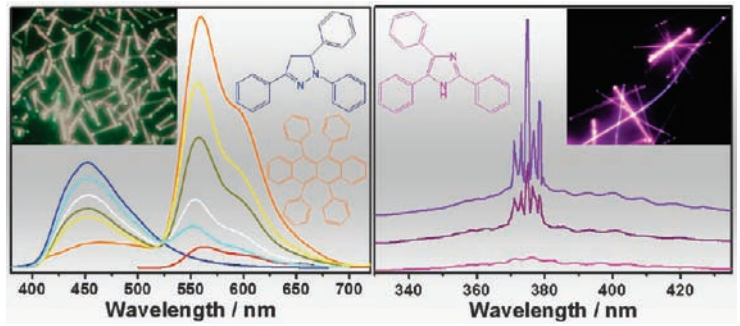

In the last 10 years, nanomaterials based on small organic molecules have attracted increasing attention. Such materials have unique optical and electronic properties, which could lead to new applications in nanoscale devices. Zero-dimensional (0D) organic nanoparticles with amorphous structures have been widely studied; however, the systematic investigation of crystalline one-dimensional (1D) organic nanostructures has only emerged in recent years.

Researchers have used inorganic 1D nanomaterials, such as wires, tubes, and belts, as building blocks in optoelectronic nanodevices. We expect that their organic counterparts will also play an important role in this field. Because organic nanomaterials are composed of molecular units with weaker intermolecular interactions, they allow for higher structural tunability, reactivity, and processability. In addition, organic materials usually possess higher luminescence efficiency and can be grown on almost any solid substrate. In this Account, we describe recent progress in our group toward the construction of organic 1D nanomaterials and studies of their unique optical and electronic properties. First, we introduce the techniques for synthesizing 1D organic nanostructures. Because this strategy is both facile and reliable, liquid phase synthesis is most commonly used. More importantly, this method allows researchers to produce composite materials, including core/sheath and uniformly doped structures, which allow to investigate the interactions between different components in the nanomaterials, including fluorescent resonance energy transfer and photoinduced electron transfer.

Physical vapor deposition allows for the synthesis of organic 1D nanomaterials with high crystallinity. Nanomaterials produced with this method offer improved charge transport properties and better optoelectronic performance in areas including multicolor emission, tunable emission, optical waveguide, and lasing. Although inorganic nanomaterials have developed rapidly, our findings highlight the importance of organic compounds as components of novel 1D nanomaterials.

1. Introduction

One-dimensional (1D) nanomaterials, including nanowires, nanotubes, nanobelts, etc., have been attracting considerable attention during the past decade,[1,2] because the two-dimensional quantum confinement effect makes them promising as building blocks for miniaturized devices, electrochemical sensors,[3] light-emitting diodes,[4] field-effect transistors,[5] solar cells,[6] and so on. Most of the relevant works, however, have been focused

Published on the Web 12/02/2009 www.pubs.acs.org/acr
10.1021/ar900219n

on inorganic materials, whereas organic ones have been much less studied in this area, although the organic functional molecules have played important roles in various optoelectronic devices.

In recent years, nanomaterials based on functional organic molecules have captured more and more interest.[7] Besides the strikingly different optoelectronic properties from those of their inorganic counterparts, organic nanomaterials also have some advantages in good doping properties,[8] high reaction activity,[9] good processability,[10] and high photoluminescence (PL) efficiency,[11] which make them complementary to the inorganic materials. Among these organic nanomaterials, one-dimensional (1D) nanostructures have been specially emphasized,[12] because they are expected to play important roles as interconnects and functional units in the next generation of miniaturized optoelectronics. In addition, crystalline 1D organic nanostructures offer better stabilities and charge transport properties and hence better optoelectronic performances of the final devices.[13] Some unique applications, like color-tunable display,[14,15] field-effect transistors,[16] chemical sensors,[17,18] optical waveguides,[19] and lasers[20] have been achieved from such organic 1D materials and have been proven to be very promising as building blocks for the miniaturized optoelectronic devices.

In this Account, we introduce the recent progress in our group on the construction and unique optoelectronic properties of nanomaterials based on functional organic molecules. Unlike the previous review article,[7] here we emphasize the construction of 1D nanostructures of high crystallinity with liquid phase and vapor phase strategies, and some more recently studied optical and electronic properties of the prepared 1D organic nanomaterials are also demonstrated.

2. Construction Strategies

The development of facile, mild, and universal construction strategies is prerequisite to the further investigations of organic 1D nanostructures. Most of the present approaches to inorganic 1D nanomaterials are not applicable for organic ones due to the lower melting and sublimation points. However, some fruitful attempts have been made in this area during the past couple of years, and in this section, we demonstrate some successful examples for the achievements of organic 1D nanomaterials by dividing them into liquid and vapor phase based methods.

Self-Assembly in Liquid Phase. Almost everything has the inclination of self-assembly. Molecular self-assembly in liquid solutions is a strategy for nanofabrication that involves designing molecules and supramolecular entities. The assembly of organic molecules to nanostructures with defined morphologies needs driving forces from the molecules themselves including hydrogen bond, $\pi-\pi$ stacking, van der Waals contact, etc. Sometimes the self-assembly process also requires induction from the surroundings like the interactions between the organic molecules and the solvents or auxiliaries.

The single crystalline nano- and submicrotubes of a small organic functional compound, 2,4,5-triphenylimidazole (TPI), were synthesized by rapid dispersion of the TPI molecules from a good solvent into a nonsolvent, water.[21] The rapid change of the surroundings induced the self-assembly of TPI molecules. Tubes with high monodispersity and open-ended structures were obtained after the assembly of TPI at different temperatures. Each tube has a well-defined 1D morphology and single crystalline structure. The length and diameter of the TPI tubs can be tuned by changing the assembly conditions. The characterization of temporal morphology evolution indicated that the tubes were obtained by the rolling and seaming of preorganized 2D lamellar structures. The results of NMR, XPS, and absorption spectra revealed that the lamellar structures were constructed via the cooperation of three chemically orthoganol and spatially independent noncovalent intermolecular interactions, that is, hydrogen bonds (H-bond), $\pi-\pi$ interactions, and van der Waals contacts as shown in Figure 1.

Template-Induced Self-Assembly in Liquid Phase. Although solvent change induced assembly is a facile method for the fabrication of 1D nanomaterials, it requires strong intermolecular interactions in the target compounds, like H-bonds or effective $\pi-\pi$ stacking. For those molecules without such strong noncovalent interactions, the 1D molecular aggregations might be directed via external forces. The template method represents a straightforward route to fabricate nanostructures by inducing the target molecules to grow according to the patterns of the templates.

It is well-known that micelles with different shapes, like spherical or rod-like, will be formed in surfactant solutions when the concentration reaches the critical micelle concentration (CMC). The rod-like micelles can be used as soft templates for the 1D assembly of organic molecules. Nanofibers of 1,3-diphenyl-2-pyrazoline (DP) were prepared through the self-assembly of DP molecules in cetyltrimethylammonium bromide (CTAB) micelles.[22] Figure 2A shows the SEM morphology of the nanofibers. The shape and size of the fibers can be controlled by changing the molar ratio of DP to CTAB. Figure 2B illustrates the formation mechanism of the fibers. The CTAB tended to form spherical micelles at lower DP/CTAB

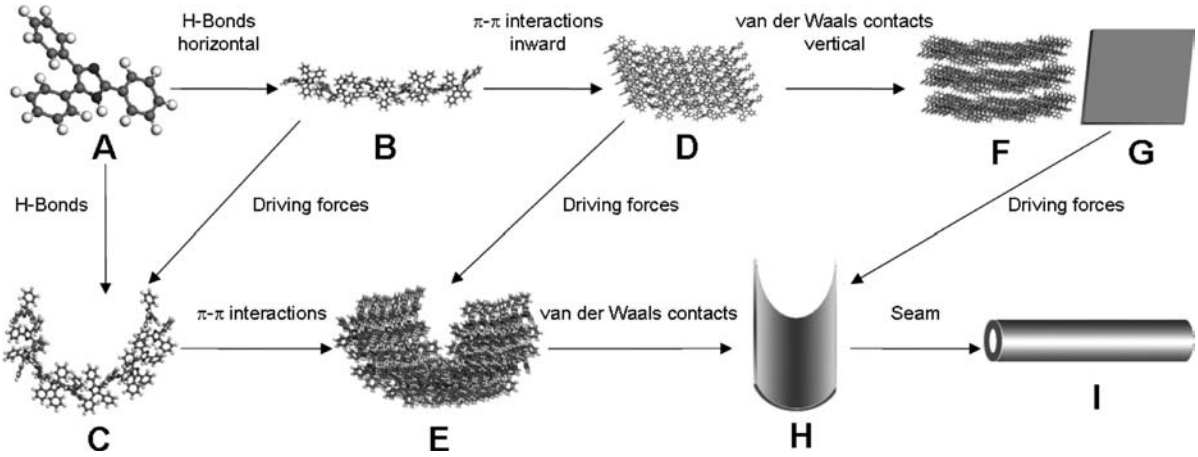

FIGURE 1. Schematic representation for the formation of TPI tubes: (A) optimized geometry of a single TPI molecule; (B, C) linear and curled motifs of TPI supramolecular H-bonded chains; (D, E) flat and curled monolayer sheets from the two motifs of chains; (F) multilayer sheet by stacking of the monolayers; (G−I) sketch maps of the multilayer flat lamellar, curled lamellar, and tubular structures, respectively.

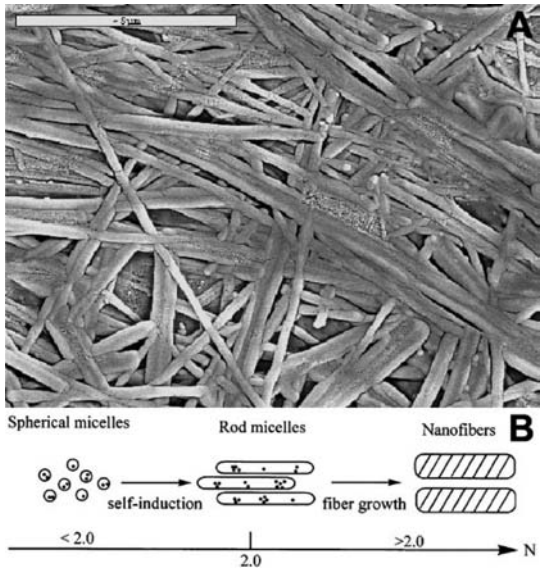

FIGURE 2. (A) SEM image of the prepared DP nanofibers (scale bar is 5 μm) and (B) representation of the formation mechanism of the DP nanofiber, in which *N* is the molar ratio of DP/CTAB.

molar ratios, while increase of the DP amount induced the sphere-to-rod transition of the micelles, which act as the template to direct the growth of DP in a 1D manner. This method was proven to be applicable to a variety of functional molecules.[23]

Besides micelles, porous membrane materials, including anodized aluminum oxide (AAO), silica, nanochannel glass, etc., are also used as templates for inducing the 1D growth of organic molecules via capillary forces. We prepared perylene[24] and dibenzoylmethane (DBM)[25] nanotubes by repeatedly immersing the porous alumina template into saturated organic solutions. Nanotubes of different sizes can be prepared by using alumina templates with different pore diameters, and the crystallinity of the products can be increased by subsequent thermal treatments.

Synthesis of Organic 1D Nanocomposites in Liquid Phase. Besides the 1D nanostructures of single composition, we demonstrated that the 1D composite nanomaterials including core/sheath and uniformly doped structures can also be achieved via self-assembly in liquid phases. First, the core/sheath nanorods were prepared by a step-by-step assembly of 1,5-diphenyl-3-(naphthalene-4-yl)-1*H*-pyrazoline (DPNP) and 2,5-bis(2-(*N*-hexadecylpyridinium-4-yl)-vinyl)pyrrole iodide (I-Py).[26] DPNP nanorods were prepared with solvent exchange, and after the nanorods were aged about 2 h, the ethanol solution of I-Py was quickly added into the nanorod dispersion under stirring. The self-assembly of I-Py molecules on the surface of the DPNP nanorods was driven by the electrostatic interaction, and therefore, core/sheath structures were obtained after aging for about 3 h (inset of Figure 3A). The PL emission spectra of the core/sheath nanorods shown in Figure 3A indicate that the contribution of I-Py composition at 590 nm increases upon increase of the aging time at the expense of that of DPNP at 470 nm, which results from fluorescent resonance energy transfer (FRET) from the DNPN core to the I-Py shell.

Uniformly doped 1D composite nanostructures were further synthesized by a simultaneous reprecipitation with an electron donor compound, 1,3,5-triphenyl-2-pyrazoline (TPP), and an electron acceptor, 1,4-dicyanonaphthalene (DCN).[27] Exciplexes were formed between TPP and DCN at the excited state in the composite nanostructures, through which the fluorescence of TPP was quenched (Figure 3B). The emission color of the nanocomposites can be tuned by changing the doping content of DCN. Theoretical calculations confirm that pho-

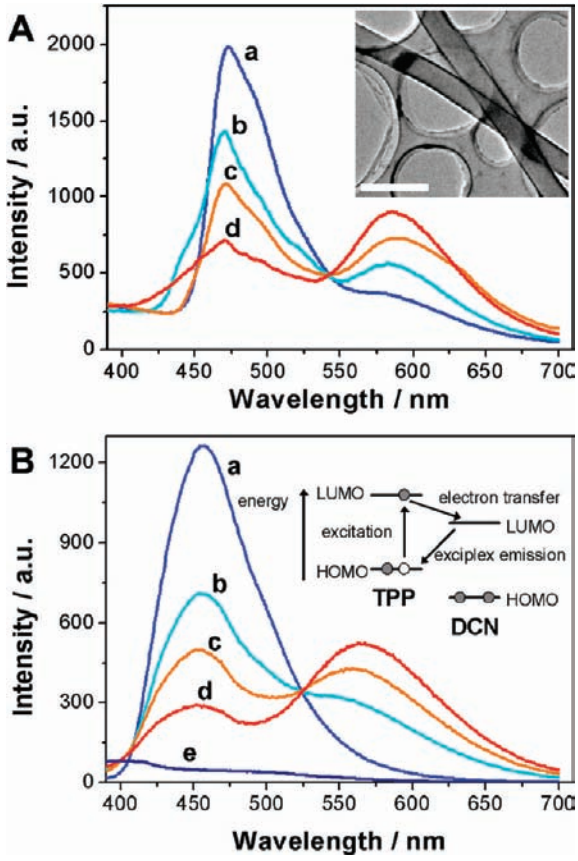

FIGURE 3. (A) PL spectra of DPNP/I-Py core/sheath nanorods obtained at different aging intervals: (a) 5; (b) 30; (c) 60; and (d) 180 min. Inset is the TEM image of the core/sheath 1D nanostructures; scale bar is 500 nm. (B) PL spectra of the 1D nanocomposite suspensions of TPP and DCN with different molar ratios in water: (a) pure TPP; (b) TPP/DCN = 4:1; (c) TPP/DCN = 2:1; (d) TPP/DCN = 1:1; and (e) pure DCN. The excitation wavelength is 365 nm. Inset is the energy level diagram representing the photoinduced electron transfer in the nanocomposites.

toinduced electron transfer (PET) occurs through an electron transition from the lowest unoccupied molecular orbital (LUMO) of the excited TPP to that of the ground-state DCN as shown in the inset of Figure 3B.

Morphology Control with Molecular Design. It has been proven that molecular structure plays an important role in the aggregation behavior of organic materials in solutions. Therefore, it is possible to control the self-assembly manner by introducing special substitute groups in the organic molecules. The facile fabrication of nanostructures with well-defined shapes from stilbazolium-like dyes was reported.[28] Stilbazolium-like dyes with different substituents were synthesized with the intention of exploring the influences of the substituent effects on the shape and therefore the optical properties of the resulting nanostructures. Self-assembly of the target molecules was induced with solvent exchange. It was found that the change of substituents influenced the morphology of

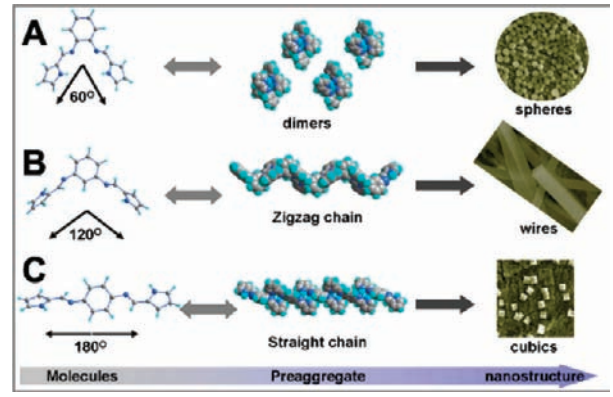

FIGURE 4. Schematic illustration for the formation processes of nanostructures from (A) *o*-, (B) *m*-, and (C) *p*-bis(iminopyrrole) benzene, respectively.

the aggregates significantly. Strong electron donor−acceptor interactions induce 1D aggregation in one compound, while spherical structures were obtained with the other compound with nonplanar structure and weak electron donor−acceptor interactions.

Besides those from derivatives with different substituents, nanostructures were also tuned between spheres, wires, and cubes via the self-assembly of three isomeric molecules of bis(iminopyrrole)benzene with same substituents on different positions.[29] Although all the three isomeric precursors, *o*-, *m*-, and *p*-bis(iminopyrrole) benzene, present similar strong multiple hydrogen-bonding interactions for molecular aggregation, distinctly shaped nanostructures were obtained. As shown in Figure 4A, the two iminopyrrole (IP) groups in the *o*-isomer are 60° open-armed. Therefore, two monomers can embed into each other to form a dimer via quadruple hydrogen bonds, which act as the basic units for the formation of spherical structures. In contrast, the configurations of *m*- and *p*-isomers, with two IP groups open-armed at an angle of 120° and 180°, respectively, determine that each molecule connects with two others via hydrogen bonds, forming chain-like structures. Also determined by molecular configuration, the chain of the *m*-isomer is zigzag shape (Figure 4B), while that of the *p*-isomer is almost linear (Figure 4C). These chains are the actual building blocks for the solid states of the two isomers to form square wires and cubes, respectively. It is the different interactions for aggregate stacking at the supramolecular level caused by the isomeric molecular structures that is responsible for the different morphological evolution.

Physical Vapor Deposition (PVD). VD is a facile and feasible method for preparing nanomaterials and has achieved great success in the synthesis of inorganic 1D nanomaterials and polymeric thin films. However, the monodispersity of the products is hard to control when small organic molecules are

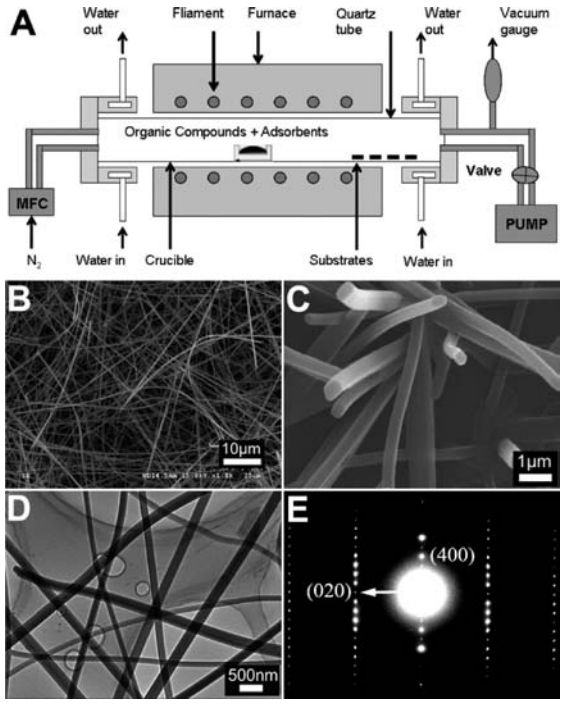

FIGURE 5. (A) Sketch of the instrument used for the adsorbent-assisted PVD; (B, C) SEM images of the TPI nanowires; (D) TEM images of some typical TPI nanowires; (E) the electron diffraction pattern of the TPI nanowire with the main diffraction spots indexed; the arrow indicates the direction of the wire.

used as deposition sources. It is known that for the VD method, the degree of saturation is the predominant factor in controlling the morphology and dispersity of the products, and it should be possible to process most solid materials into 1D nanostructures by controlling the vapor saturation at a low level.

In our recent works,[30] adsorbents such as neutral aluminum oxide or silica gel used widely in column chromatography were introduced into the PVD method (Figure 5A) to control the degree of saturation considering that there should exist an adsorption−desorption equilibrium between the adsorbents and the organic sources. The adsorbent-assisted PVD has been proven to be a general method for the synthesis of organic 1D nanomaterials with high crystallinity. Through this method, single crystalline nanowires were first prepared from a chemiluminescent compound, 2,4,5-triphenylimidazole (TPI). The SEM images of the TPI nanowires displayed in Figure 5B indicate that each nanowire has a smooth surface and uniform width all through the entire length. The SEM images of some wires growing out of the substrate surface (Figure 5C) show very flat and smooth end surfaces of the nanowire quadrangular cross sections. The TEM images in Figure 5D prove that the geometrical shape of the TPI nanostructures is a solid wire without obvious structural defects. The electron diffraction (Figure 5E) pattern reveals that each single wire has single crystalline structure and grows along the *b* axis of the TPI crystal, which was further proven by the XRD measurements. The TGA measurements proved that the adsorbents decreased the sublimation temperature and slowed the weight loss of TPI, through which the degree of saturation was well controlled and the uniformity of the nanowires was remarkably improved.

3. Optoelectronic Properties

One of the most important reasons organic 1D nanomaterials have been attracting so much attention is that their optical and electronic properties are fundamentally different from their inorganic counterparts, because the intermolecular interactions in organic materials are basically of weak types. In this section, we give an overview of the present studies on the unique optoelectronic performances of organic 1D nanostructures.

Multicolor Emission. Multicolor emissions, especially red−green−blue (RGB) emissions are essential to display and flat screens. Generally, multicolor emissions are realized with blends of dyes emitting red, green, and blue lights. Recently, we demonstrated multicolor emissions with the 1D nanostructures of a single organic compound.[14] The selected model compound, 1,2,3,4,5-pentaphenyl-1,3-cyclopentadiene (PPCP), is a blue light-emitting dye used in electroluminescence devices. After being fabricated to crystalline 1D nanostructures, PPCP displayed a multicolor emission property, that is, blue, green, and red emissions were achieved by exciting the same sample with appropriate wavelengths.

As is shown in the inset of Figure 6, only a deep blue emission with a maximum at 453 nm was observed from PPCP monomers in ethanol solution at room temperature. Comparatively, the vibronic levels are well resolved in the low-temperature spectrum measured at 77 K, which results from the decrease of the degree of freedom of molecular vibrations and the increase of molecular orientation. It is interesting to note that the narrowing spectrum can also be observed in the PPCP nanostructures even at room temperature. A more important result shown in Figure 6 is the multicolor emission from the PPCP nanomaterials. Three different emission colors of blue, green, and red were achieved by exciting the nanostructures with UV (330 nm), blue (450 nm), and green light (550 nm), respectively. The green and red emission spectra also present well-resolved vibrational fine structures. The quantum yields of the blue, green, and red emissions are 0.23, 0.15, and 0.08, respectively. The comparison between the emissions

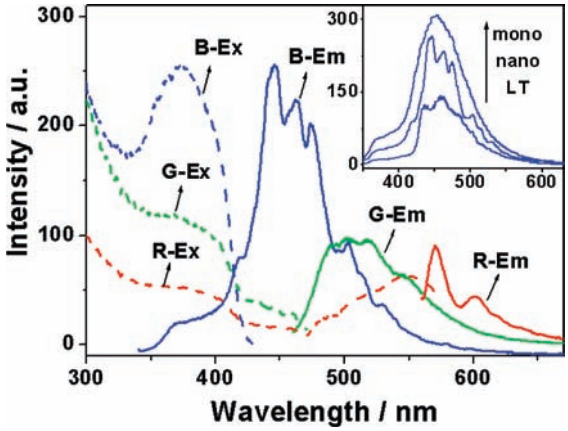

FIGURE 6. Solid lines indicate the blue (B), green (G), and red (R) fluorescence emission (Em) spectra of the PPCP nanomaterials excited with 330, 450, and 550 nm light, respectively. Dashed lines indicate the corresponding excitation (Ex) spectra monitored with blue (460 nm), green (520 nm), and red (600 nm) emissions, respectively. The inset shows the room-temperature fluorescence emission spectra of PPCP monomers in ethanol solution (mono) and nanomaterials deposited onto quartz wafers (nano) and the low-temperature (LT) fluorescence spectrum of PPCP monomers at 77 K.

from the crystalline nanostructure with those of the amorphous thin films testified that the green and red emitting centers in the PPCP nanomaterials were induced by their crystallinity and the structural defect energy levels therein. Meanwhile, the emission from each center can be further enhanced by the 1D structure of the nanomaterials by the self-convergence along specific directions.

Electroluminescence and Field Emission. Since its strong electroluminescence with a low driving voltage was reported, tris(8-hydroxyquinoline)aluminum (Alq_3) has played an important role in organic light-emitting diodes (OLEDs). In our work, Alq_3 nanowires were prepared with the adsorbent-assisted PVD method, and the nanowires were then applied in LED and field emission devices.[31] The *I*−*V* characteristics indicate a typical diode-like behavior of the devices. Figure 7A displays the luminance−voltage characteristics of the LED devices prepared from Alq_3 nanowires with different diameters. It can be seen that the performance the Alq_3 nanowire-based LEDs shows an obvious size-dependent effect. The turn-on voltages of the device from Alq_3 nanowires with diameter of 40 nm is about 1 V lower than that of the one from nanowires 60 nm in diameter, and the current efficiency of the former is higher by 20%. When the driving voltage is 12.5 V, the external quantum efficiencies of the devices based on nanowires with diameter of 40, 60 and 80 nm are 0.90%, 0.58%, and 0.28%, respectively.

Another important optoelectronic property of the Alq_3 nanowires is the field emission with a relatively low turn-on

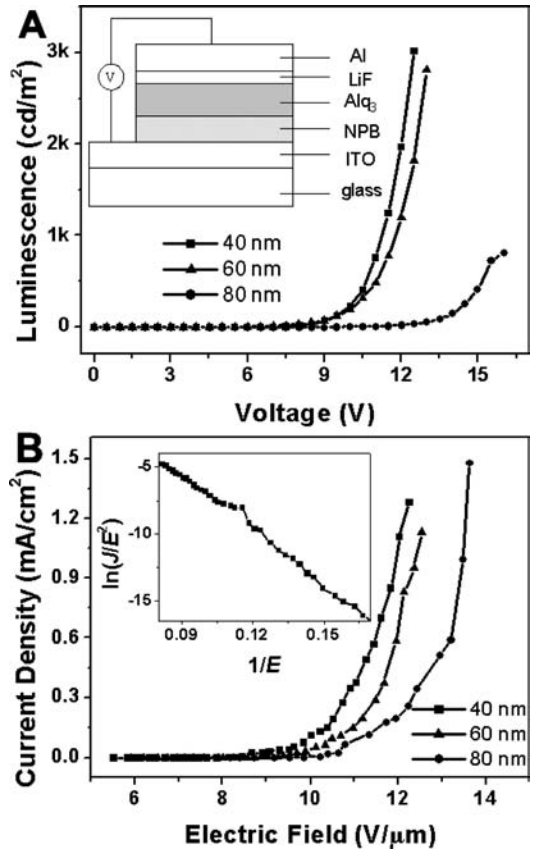

FIGURE 7. (A) Luminance−voltage characteristics of the LEDs fabricated from Alq_3 nanowires with average diameters of 40, 60, and 80 nm. The inset shows the schematic structure of the devices. (B) Field-emission *J*−*E* curves of the Alq_3 nanowires with different diameters. The insert shows the Fowler−Nordheim plot of nanowires with average diameter of 40 nm, which yields a straight line with a slope of about −135.

field, which also shows a size-dependent performance. Figure 7B displays the field emission *J*−*E* curves of the Alq_3 nanowires with different diameters. With the diameter decreasing from 80 to 40 nm, the turn-on field decreased from 10.3 to 8.5 V/μm and the threshold field decreased from 13.5 to 11.6 V/μm. The turn-on field here is lower than that of the amorphous Alq_3 nanowires due to the high degree of crystallinity.

Organic Nanotube Optical Waveguides. The tubular 1D nano- and submicrostructures were synthesized from 9,10-bis(phenylethynyl)anthracene (BPEA),[32] an emitting dye with very high luminescence efficiency. The organic molecules were first exchanged into boiling water, where the molecules are dissolved, and then self-assembly of the molecules was induced by programmed cooling of the whole system at different speeds. As shown in Figure 8A, the PL microscopy image of the BPEA tubes on quartz substrates exhibited a characteristic green to yellow emission, with very bright luminescence spots at both tips of each tube and relatively weaker

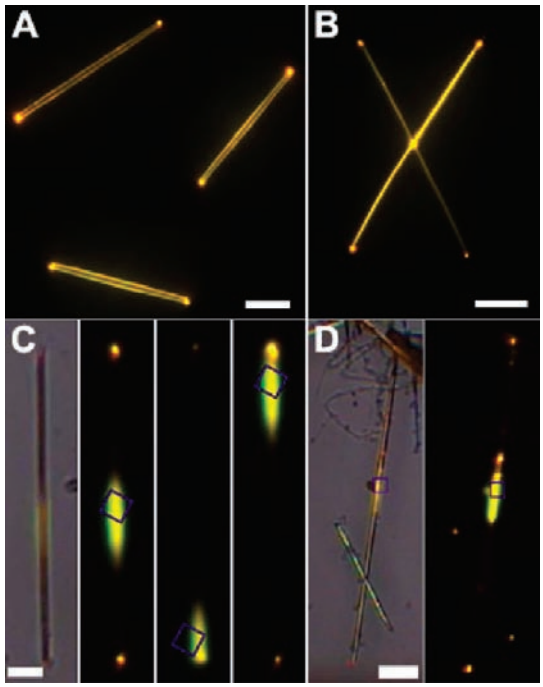

FIGURE 8. PL microscopy images of (A) some isolated BPEA tubes and (B) two crossed tubes. Both samples were excited with blue light in 460−490 nm region. Scale bars are 20 μm. (C) Bright-field image and microarea PL images obtained by exciting the identical tube at three different positions; scale bar is 10 μm. (D) Bright-field and microarea PL images of two crossed tubes; scale bar is 20 μm. The blue squares indicate the excited positions.

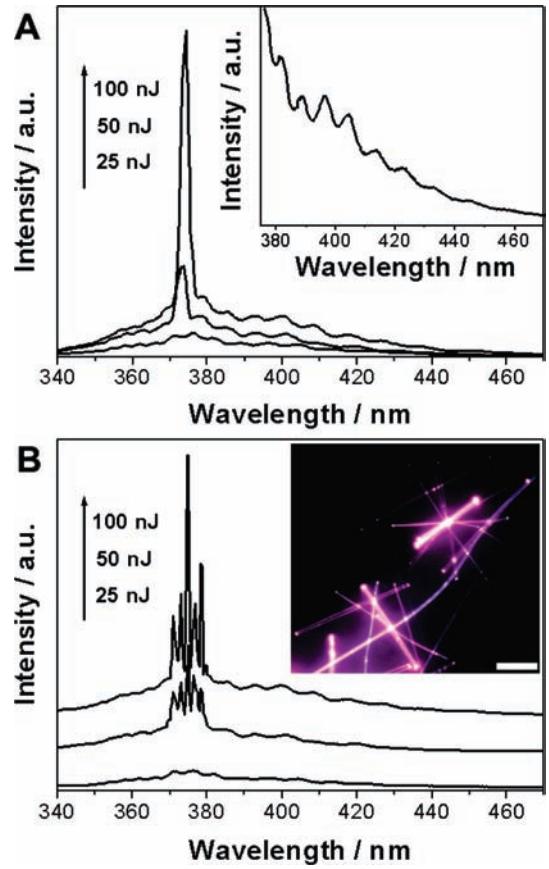

FIGURE 9. (A) Power-dependent emission spectra recorded on the tip of a TPI wire with 400 nm width and 15 μm length. The inset shows the expansion of the higher wavelength region with resolved modes. (B) Power-dependent emission spectra recorded on the tip of a TPI wire with width of 800 nm and length of 15 μm. The inset shows the PL microscopy image of TPI nanowires deposited onto quartz wafers. Scale bar is 10 μm.

emission from the tube bodies, which is a typical characteristic of an optical waveguide. Almost all of the observed tubes reveal this kind of waveguide behavior. Figure 8C indicates that the 1D BPEA tubes can serve as active optical waveguides that allow the locally excited PL to propagate along the length of the 1D structures and out-couple at the tube tips. In addition, when the excitation light is input from one of the two crossed tubes, the emissions can be coupled to the other tubes, as shown in Figure 8B,D. The refractive index of the BPEA is ∼1.65, and that of the quartz substrates is ∼1.5 at the measured wavelength. The small difference between the two refractive indexes results in a considerable energy leakage in the case of the solid BPEA microrods. However, in the tubular structures here, the light can be propagated at the interface of BPEA and the air inside the tube, whose refractive index is ∼1, and therefore the optical loss was significantly eliminated.

Lasing from Organic Nanowires. The nanoscale waveguides and laser sources are essential to the integrated nanophotonic systems and are crucial for optical information processing. Inorganic semiconductor 1D nanomaterials have been adopted as optical pumped lasers, and the microcavity effects and optically pumped lasing in nanowires based on conjugated polymers were also studied.[20] In our recent work, we proved that the nanowire waveguides and lasers can also be extended to small organic molecules.[33] The TPI nanowires mentioned above in Figure 5 revealed obvious fluorescence narrowing spectra at room temperature. The single crystalline wires can behave as nanoscale active optical waveguides, and optically pumped lasing was also observed from single nanowires with increase of the excitation power.

The PL microscopy image of the TPI nanowires (inset of Figure 9B) shows that the wires reveal good waveguide properties. An isolated single TPI nanowire was excited with a pulsed laser with 325 nm wavelength, and the emissions were collected from the tip area. Figure 9A gives the power-dependent PL spectra recorded from the tip of a wire with 400 nm width and 15 μm length. It indicates that PL modulations emerge on the lower energy side of the emission band, which can be observed more clearly from the inset. The modes do not occur at the short wavelength side because of photon

reabsorption. At low excitation power, the structure displays a broad and featureless emission at about 375 nm. Above a threshold, amplified spontaneous emission was observed, which is indicated by the appearance of sharp cavity modes above an onset power. The energy dependence of the luminescent intensity and fwhm of the emission spectra reveal a nonlinear gain and a threshold characteristic of the laser. Below the threshold, the PL intensity increases almost linearly with the excitation power, and once the critical pumped energy is reached, there emerges a kink in the power dependence of emission intensity, which results in a large increased gain.

The transition from the spontaneous PL to the stimulated emission is significantly influenced by the size of the nanowires. For thinner wires with width of 200 nm, no emission was detected due to the lack of resonator property. On the other hand, if the wire length is too small, even when the width is large enough, the stimulated emission cannot be observed either, although the PL intensity is also enhanced on the increase of the pump energy. This is because the high degree of spontaneous emission coupling in small mode volume will result in a broad cavity mode. When both the length and the width of the wire are large enough, multimode lasing can be observed as shown in Figure 9B.

Tunable Emission from Binary Organic Nanowires. Binary doped organic nanowires were prepared with the above-mentioned adsorbent-assisted PVD method. A blue light emitter, 1,3,5-triphenyl-2-pyrazoline (TPP), and rubrene, a good orange dye used as the dopant in host/guest OLEDs with good transport property, were chosen as the model compounds, which were fabricated into uniformly doped crystalline nanorods and nanowires with the adsorbent-assisted PVD method.[15] The doping content was tuned by changing the molar ratio of the two sources.

Figure 10A−C shows the fluorescence microscopy images of the binary nanostructures with various doping contents. The homogeneous emission color from all of the nanorods/wires in each sample testified that rubrene crystal grains were dispersed uniformly into the TPP matrices. The binary nanowires also show waveguide properties, which is proven by the microarea fluorescence microscopy of single nanorod in Figure 10C. It is revealed by the fluorescence microscopy images that the emission color evolves from blue to orange with the increase of rubrene content and, more importantly, white emission can be achieved when a proper TPP/rubrene molar ratio (100:1) is adopted. The tunable emission can also be

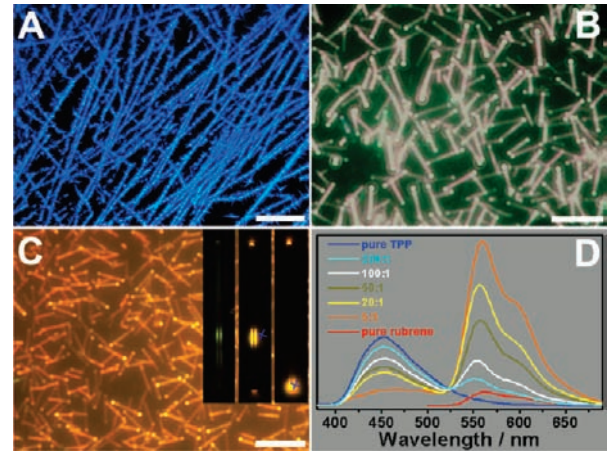

FIGURE 10. Fluorescence microscopy images of 1D nanomaterials with different rubrene contents: (A) pure TPP, excited with UV (330−385 nm); (B) 100:1 TPP/rubrene, excited with UV; (C) pure rubrene, excited with blue light (460−490 nm). Scale bars are 5 μm. Insets are the bright-field image (left) and microarea fluorescence images of a single nanorod obtained by exciting the middle part (middle) and top area (right) using a focused laser; the blue crosses indicate the excited position. (D) Emission spectra of the binary nanomaterials deposited onto quartz wafers with different TPP/rubrene molar ratios.

observed from the evolution of the fluorescence spectra of the nanostructures with the change of rubrene content shown in Figure 10D.

For comparison, doped amorphous thin films were also prepared with the coevaporation technique. The colors of the doped films are not stable because of the oxidation of rubrene. In contrast, the emission colors of the binary nanowires are very stable, which was ascribed to the crystallinity of rubrene. In the amorphous films, the emission of TPP can be quenched almost completely at 4% rubrene doping content, which is caused by the higher energy transfer efficiency. In contrast, the emission of TPP cannot be quenched completely even when the dopant content was as high as 20% in the doped nanowires. Both the color stability and the incomplete quenching are essential to the realization of white-light emission.

Waveguide Modulator from Binary Organic Nanotubes. Very recently, we prepared binary tubular structures with high crystallinity, in which perylene molecules are doped in the matrix of TPI.[34] As shown in Figure 11A, hexagonal hollow tubes with lengths of ~100 μm were obtained. The measurements of PL microscopy, as well as the spatially resolved PL spectra of a single tube (Figure 11B), indicate that the tubes present typical features of an optical waveguide, in which the PL of TPI at 402 nm shows a constant loss coefficient of 97 dB/mm, which those from perylene as a result of intermolecular fluorescence resonance energy transfer (IFRET) reveal

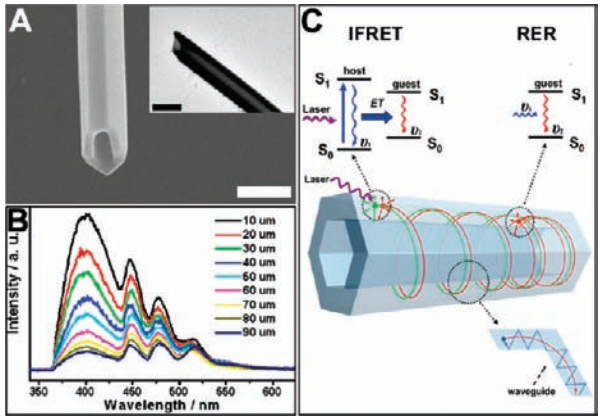

FIGURE 11. (A) SEM and TEM images of a single perylene-doped TPI tube. Scale bars are 1 μm. (B) Spatially resolved PL spectra of out-coupled light for a single binary tube recorded by excitation at a distance of 10−90 mm from the tip. (C) A schematic representation of the annular cavity of the binary mictotube and energy diagrams for the IFRET and RER processes.

nonlinear losses, and the optical loss at the longer wavelength is approximately zero.

It was also observed that the out-coupled PL redistributes from short to long wavelengths during the propagation, making the microtube act as a waveguide modulator. The hollow structure is considered to be responsible for the waveguide modulation, as is shown in Figure 11C. The air medium inside the tubes leads to spatial confinement of photons in two dimensions in the tube wall, which forms an annular microcavity. light traveling round and round the annular cavity (see the bottom image of Figure 11C) results in a much longer propagation length in the microtube than that in the solid structures. The waveguide modulation in the binary tube is a result of the reabsorption of the UV photon from the TPI matrix by the doped perylene component and subsequent reemission of a green photon, which is a remote energy relay (RER) process.

4. Conclusion and Perspectives

In this Account, we summarized some recent progress in the synthesis and optoelectronic properties of 1D nanomaterials based on small organic functional molecules. Compared with the 0D nanoparticles, the construction of 1D organic nanostructures used to be a challenge in materials science. This is especially true for those with single crystal structures, which would offer better optoelectronic performances to the nanomaterials and to the final devices. First, we introduced some facile liquid and vapor phase based synthesis methods, which are suitable for the preparation of both solid and hollow nanostructures. Moreover, composite 1D nanomaterials including core/sheath and well-controlled doped materials can also be achieved. Second, we demonstrated the unique optical and electronic properties of the constructed organic 1D nanostructures, including multicolor emission, tunable emission, optical waveguide, lasing, etc., which result from the weak intermolecular interactions or their molecular crystal structures.

At present, the development of organic low-dimensional materials still lags far behind that of their inorganic counterparts, although considerable attention has been paid to this area in the past couple of years. People still have heavy responsibilities for the exploration in this field. First, to further improve the optoelectronic properties of the organic 1D nanostructures, none of these is dispensable: the design and synthesis of novel optofunctional molecules, the successful construction of nanomaterials with desired structures from the synthesized molecules, and then the powerful characterization of the constructed materials. More importantly, to realize the full potential of applications, the 1D building blocks should be more efficiently integrated into devices of various optoelectronic functions.

This work was supported by National Natural Science Foundation of China (Grant Nos. 20733006, 20803086), the Chinese Academy of Sciences, and National Basic Research Program of China (Grant No. 2006CB806202).

BIOGRAPHICAL INFORMATION

Yong Sheng Zhao received his Ph.D. degree in 2006 at the Institute of Chemistry, Chinese Academy of Sciences (ICCAS). After that, he joined Prof. Qibing Pei's laboratory at the University of California at Los Angeles (UCLA) and then Prof. Jiaxing Huang's group at Northwestern University as a postdoctoral fellow. In 2009, he returned to ICCAS as a Professor of Chemistry. His research interests include photonic and electronic properties of organic nanomaterials and organic/inorganic hybrid nanomaterials.

Hongbing Fu received his Ph.D. degree in 2001 at ICCAS, where he is now a Professor of Chemistry. His research focuses on organic low-dimensional electronics.

Aidong Peng received his Ph.D. degree in 2005, and he is currently working on doped organic nanomaterials as an associate professor in ICCAS.

Ying Ma received her Ph.D. degree at the Institute of Photographic Chemistry, CAS, in 1999. She is currently an associate professor in ICCAS on semiconductor nanomaterials.

Qing Liao received his Ph.D. degree in 2007 at ICCAS. He is currently a research associate in Prof. Jiannian Yao's group, working on optoelectronics of self-assembled molecules.

Jiannian Yao received his Ph.D. degree with Prof. Akira Fujishima at Tokyo University in 1993. He joined the Institute of Photographic Chemistry, CAS, in 1995, and now he is a Professor of

Chemistry and Materials Science in ICCAS. He is currently serving as a permanent member and general secretary of the Chinese Chemical Society (CCS) and the vice president of the National Natural Science Foundation of China (NSFC). His research interests are focused on optofunctional materials.

FOOTNOTES

*To whom correspondence should be addressed. E-mail: jnyao@iccas.ac.cn.

REFERENCES

1 Hu, J.; Odom, T. W.; Lieber, C. M. Chemistry and physics in one dimension: Synthesis and properties of nanowires and nanotubes. *Acc. Chem. Res.* **1999**, *32*, 435–445.

2 Xia, Y.; Yang, P.; Sun, Y.; Wu, Y.; Mayers, B.; Gates, B.; Yin, Y.; Kim, F.; Yan, H. One-dimensional nanostructures: Synthesis, characterization, and applications. *Adv. Mater.* **2003**, *15*, 353–389.

3 Wang, Z. L. Nanobelts, nanowires and nanodiskettes of semiconducting oxides - from materials to nanodevices. *Adv. Mater.* **2003**, *15*, 432–436.

4 Könenkamp, R.; Word, R. C.; Godinez, M. Ultraviolet electroluminescence from ZnO/polymer heterojunction light-emitting diodes. *Nano Lett.* **2005**, *5*, 2005–2008.

5 Goldberger, J.; Hochbaum, A.; Fan, R.; Yang, P. Vertical silicon nanowire field effect transistors. *Nano Lett.* **2006**, *6*, 973–977.

6 Law, M.; Greene, L. E.; Johnson, J. C.; Saykally, R.; Yang, P. Nanowire dye-sensitized solar cells. *Nat. Mater.* **2005**, *4*, 455–459.

7 Zhao, Y. S.; Fu, H.; Peng, A; Ma, Y.; Xiao, D.; Yao, J. Low-dimensional nanomaterials based on small organic molecules: Preparation and optoelectronic properties. *Adv. Mater.* **2008**, *20*, 2859–2876.

8 Peng, A.; Xiao, D.; Ma, Y.; Yang, W.; Yao, J. Tunable emission from doped 1,3,5-triphenyl-2-pyrazoline organic nanoparticles. *Adv. Mater.* **2005**, *17*, 2070–2073.

9 Zhao, Y. S.; Wu, J.; Huang, J. Vertical organic nanowire arrays: Controlled synthesis and chemical sensors. *J. Am. Chem. Soc.* **2009**, *131*, 3158–3159.

10 An, B. -K.; Kwon, S. -K.; Park, S. Y. Photopatterned arrays of fluorescent organic nanoparticles. *Angew. Chem., Int. Ed.* **2007**, *46*, 1978–1982.

11 An, B. -K.; Kwon, S. -K.; Jung, S. -D.; Park, S. Y. Enhanced emission and its switching in fluorescent organic nanoparticles. *J. Am. Chem. Soc.* **2002**, *124*, 14410–14415.

12 Zang, L.; Che, Y.; Moore, J. S. One-dimensional self-assembly of planar π-conjugated molecules: Adaptable building blocks for organic nanodevices. *Acc. Chem. Res.* **2008**, *41*, 1596–1608.

13 Fardy, M.; Yang, P. Lilliputian light sticks. *Nature* **2008**, *451*, 408–409.

14 Zhao, Y. S.; Fu, H.; Hu, F.; Peng, A.; Yao, J. Multicolor emission from ordered assemblies of organic 1D nanomaterials. *Adv. Mater.* **2007**, *19*, 3554–3558.

15 Zhao, Y. S.; Fu, H.; Hu, F.; Peng, A.; Yang, W.; Yao, J. Tunable emission from binary organic one-dimensional nanomaterials: an alternative approach to white-light emission. *Adv. Mater.* **2008**, *20*, 79–83.

16 Briseno, A. L.; Mannsfeld, S. C. B.; Lu, X.; Xiong, Y.; Jenekhe, S. A.; Bao, Z.; Xia, Y. Fabrication of field-effect transistors from hexathiapentacene single-crystal nanowires. *Nano Lett.* **2007**, *7*, 668–675.

17 Naddo, T.; Che, Y.; Zhang, W.; Balakrishnan, K.; Yang, X.; Yen, M.; Zhao, J.; Moore, J. S.; Zang, L. Detection of explosives with a fluorescent nanofibril film. *J. Am. Chem. Soc.* **2007**, *129*, 6978–6979.

18 Che, Y.; Yang, X.; Loser, S.; Zang, L. Expedient vapor probing of organic amines using fluorescent nanofibers fabricated from an n-type organic semiconductor. *Nano Lett.* **2008**, *8*, 2219–2223.

19 Takazawa, K.; Kitahama, Y.; Kimura, Y.; Kido, G. Optical waveguide self-assembled from organic dye molecules in solution. *Nano Lett.* **2005**, *5*, 1293–1096.

20 O'Carroll, D.; Lieberwirth, I.; Redmond, G. Microcavity effects and optically pumped lasing in single conjugated polymer nanowires. *Nat. Nanotechnol.* **2007**, *2*, 180–184.

21 Zhao, Y. S.; Yang, W.; Xiao, D.; Sheng, X.; Yang, X.; Shuai, Z.; Luo, Y.; Yao, J. Single crystalline submicrotubes from small organic molecules. *Chem. Mater.* **2005**, *17*, 6430–6435.

22 Fu, H.; Xiao, D; Yao, J.; Yang, G. Nanofibers of 1,3-diphenyl-2-pyrazoline induced by cetyltrimethylammonium bromide micelles. *Angew. Chem., Int. Ed.* **2003**, *42*, 2883–2886.

23 Hu, J. -S.; Guo, Y. -G.; Liang, H. -P.; Wan, L. -J.; Jiang, L. Three-dimensional self-organization of supramolecular self-assembled porphyrin hollow hexagonal nanoprisms. *J. Am. Chem. Soc.* **2005**, *127*, 17090–17095.

24 Zhao, L.; Yang, W.; Ma, Y.; Yao, J.; Li, Y.; Liu, H. Perylene nanotubes fabricated by the template method. *Chem. Commun.* **2003**, 2442–2443.

25 Zhao, L.; Yang, W.; Luo, Y.; Zhai, T.; Zhang, G.; Yao, J. Nanotubes from isomeric dibenzoylmethane molecules. *Chem.—Eur. J.* **2005**, *11*, 3773–3778.

26 Kang, L.; Chen, Y.; Xiao, D.; Peng, A.; Shen, F.; Kuang, X.; Fu, H.; Yao, J. Organic core/diffuse-shell nanorods: Fabrication, characterization and energy transfer. *Chem. Commun.* **2007**, 2695–2697.

27 Shen, F.; Peng, A.; Chen, Y.; Dong, Y.; Jiang, Z.; Wang, Y,; Fu, H.; Yao, J. Photoinduced electron transfer in coaggregates of dicyanonaphthalene and pyrazoline. *J. Phys. Chem. A* **2008**, *112*, 2206–2210.

28 Tian, Z.; Chen, Y.; Yang, W.; Yao, J.; Zhu, L.; Shuai, Z. Low-dimensional aggregates from stilbazolium-like dyes. *Angew. Chem., Int. Ed.* **2004**, *43*, 4060–4063.

29 Wang, Y.; Fu, H.; Peng, A.; Zhao, Y.; Ma, J.; Ma, Y.; Yao, J. Distinct nanostructures from isomeric molecules of bis(iminopyrrole) benzenes: effects of molecular structures on nanostructural morphologies. *Chem. Commun.* **2007**, 1623–1625.

30 Zhao, Y. S.; Xiao, D.; Yang, W.; Peng, A.; Yao, J. 2,4,5-Triphenylimidazole nanowires with fluorescence narrowing spectra prep ared through the adsorbent-assisted physical vapor deposition method. *Chem. Mater.* **2006**, *18*, 2302–2306.

31 Zhao, Y. S.; Di, C. A.; Yang, W.; Yu, G.; liu, Y.; Yao, J. Photoluminescence and electroluminescence from tris(8-hydroxyquinoline)aluminum nanowires prepared by adsorbent-assisted physical vapor deposition. *Adv. Funct. Mater.* **2006**, *16*, 1985–1991.

32 Zhao, Y. S.; Xu, J.; Peng, A.; Fu, H.; Ma, Y.; Jiang, L.; Yao, J. Optical waveguide based on crystalline organic microtubes and microrods. *Angew. Chem., Int. Ed.* **2008**, *47*, 7301–7305.

33 Zhao, Y. S.; Peng, A.; Fu, H.; Ma, Y.; Yao, J. Nanowire waveguides and ultraviolet lasers based on small organic molecules. *Adv. Mater.* **2008**, *20*, 1661–1665.

34 Liao, Q.; Fu, H.; Yao, J. Waveguide modulator by energy remote relay from binary organic crystalline microtubes. *Adv. Mater.* **2009**, *21*, 4153–4157.